



## Immunoinformatics-guided designing of epitope-based subunit vaccines against the SARS Coronavirus-2 (SARS-CoV-2)



Bishajit Sarkar<sup>a,\*</sup>, Md. Asad Ullah<sup>a</sup>, Fatema Tuz Johora<sup>a</sup>, Masuma Afrin Taniya<sup>b</sup>, Yusha Araf<sup>c</sup>

<sup>a</sup> Department of Biotechnology and Genetic Engineering, Faculty of Biological Sciences, Jahangirnagar University, Dhaka, Bangladesh

<sup>b</sup> Department of Microbiology, School of Life Sciences, Independent University, Dhaka, Bangladesh

<sup>c</sup> Department of Genetic Engineering and Biotechnology, School of Life Sciences, Shahjalal University of Science and Technology, Sylhet, Bangladesh

### ARTICLE INFO

#### Keywords:

COVID-19

Coronavirus

SARS-CoV-2

Reverse vaccinology

Vaccine

Immunoinformatics

### ABSTRACT

SARS Coronavirus-2 (SARS-CoV-2) pandemic has become a global issue which has raised the concern of scientific community to design and discover a counter-measure against this deadly virus. So far, the pandemic has caused the death of hundreds of thousands of people upon infection and spreading. To date, no effective vaccine is available which can combat the infection caused by this virus. Therefore, this study was conducted to design possible epitope-based subunit vaccines against the SARS-CoV-2 virus using the approaches of reverse vaccinology and immunoinformatics. Upon continual computational experimentation, three possible vaccine constructs were designed and one vaccine construct was selected as the best vaccine based on molecular docking study which is supposed to effectively act against the SARS-CoV-2. Thereafter, the molecular dynamics simulation and *in silico* codon adaptation experiments were carried out in order to check biological stability and find effective mass production strategy of the selected vaccine. This study should contribute to uphold the present efforts of the researches to secure a definitive preventative measure against this lethal disease.

### 1. Introduction

Coronaviruses are a group of viruses that belong to the family, Coronaviridae and the order, Nidovirales. These viruses are enveloped, single stranded, positive sense RNA viruses with the genome size ranging from 26 to 32 kilobases in length. Coronaviruses infect humans as well as some other animals such as murine, porcine, feline, bovine, avian and are known to cause acquired acute upper respiratory tract infections and severe respiratory infections in children and adults (Su et al., 2016; Weiss and Navas-Martin, 2005; Masters and Perlman, 2013). Seven different human coronaviruses (HCoVs) have been identified so far. Among them, four HCoVs *i.e.*, HCoV-OC43, HCoV-229E, HCoV-NL63, and HCoV-HKU1 cause common cold in immunocompromised individuals and two other HCoVs *i.e.*, severe acute respiratory syndrome coronavirus (SARS-CoV) and Middle East respiratory syndrome coronavirus (MERS-CoV) cause severe respiratory diseases (van der Hoek et al., 2004; Hamre and Procknow, 1966; Drosten et al., 2003; Zaki et al., 2012). The severe acute respiratory syndrome coronavirus-2 (SARS-CoV-2), which is responsible for the recent pandemic all over the world, is the seventh strain known to infect human and causes the lethal coronavirus disease-2019 (COVID-19).

In December 2019, the COVID-19 was first identified in a cluster of patients with pneumonia in Wuhan, China (Peeri et al., 2020). First fatality

case due to COVID-19 was reported on 11th January 2020 in Wuhan, China and first infected case outside China was reported in Thailand on 13th January 2020 (Wang et al., 2020). The most common symptoms at onset of COVID-19 are fever, cough, fatigue, diarrhoea and in severe conditions patients face difficulties in breathing (Huang et al., 2020). World Health Organization (WHO) declared COVID-19 as pandemic on 11th March 2020, as by the end of February 2020, the infected cases outside China increased 13 fold and more than 4000 fatality cases were reported globally (World Health Organization., 2020). At the time of writing, as of 29th March 2020, 652,079 infected cases, 30,313 death cases, 137,319 recovery cases were recorded globally in 177 countries (Hopkins, 2020).

To date, there is no effective vaccine that can combat the SARS-CoV-2 infections and hence the treatments are only supportive. Use of interferons in combination with Ribavirin is somewhat effective. However, the effectiveness of combined remedy needs to be further evaluated (Fehr and Perlman, 2015). This experiment was carried out to design novel epitope-based vaccine against four proteins of SARS-CoV-2 *i.e.*, nucleocapsid phosphoprotein which is responsible for genome packaging and viral assembly (Chang et al., 2014); surface glycoprotein that is responsible for membrane fusion event during viral entry (Petit et al., 2005; Cavanagh, 1995); ORF3a protein that aids in the viral replication, characterized virulence, viral spreading and infection (Siu et al., 2019) and membrane glycoprotein

\* Corresponding author.

E-mail address: [sarkarbishajit@gmail.com](mailto:sarkarbishajit@gmail.com) (B. Sarkar).

<https://doi.org/10.1016/j.imbio.2020.151955>

Received 29 March 2020; Accepted 2 May 2020

Available online 11 May 2020

0171-2985/ © 2020 Elsevier GmbH. All rights reserved.

which mediates the interaction of virions with cell receptors (Rottier, 1995), using the approaches of reverse vaccinology and immunoinformatics.

Reverse vaccinology and immunoinformatics refer to the processes of developing vaccines where the novel antigens of a virus or micro-organism or a pathogenic organism are detected by analyzing the genomic and genetic information of that particular entity. In reverse vaccinology, the tools of bioinformatics are used for identifying and analyzing these novel antigens. These tools are used to dissect the genome and genetic makeup of a pathogen for developing a potential vaccine. Reverse vaccinology approach of vaccine development also allows the scientists to easily understand the antigenic segments of a virus or pathogen that should be given more emphasis during the vaccine development process. These methods of vaccine development are quick, cheap, efficient, easy and cost-effective way to design vaccines. These methods have been successfully used for developing vaccines to fight against many viruses *i.e.*, the Zika virus, Chikungunya virus *etc.* (Chong and Khan, 2019; María et al., 2017).

## 2. Materials and methods

The current experiment was conducted to develop potential vaccines against the SARS-CoV-2, by exploiting the strategies of reverse vaccinology and immunoinformatics (Fig. 1). The materials and methods used in this experiment were taken and adapted from the works of Ullah et al. (2020a).

## 3. Results

### 3.1. Identification, selection and retrieval of viral protein sequences

The SARS-CoV-2 was identified from the NCBI database (<https://www.ncbi.nlm.nih.gov/>). Four protein sequences *i.e.*, Nucleocapsid Phosphoprotein (accession no: QHD43423.2), Membrane Glycoprotein (accession no: QHD43419.1), ORF3a Protein (accession no: QHD43417.1) and Surface Glycoprotein (accession no: QHD43416.1) were selected for the possible vaccine construction and retrieved from

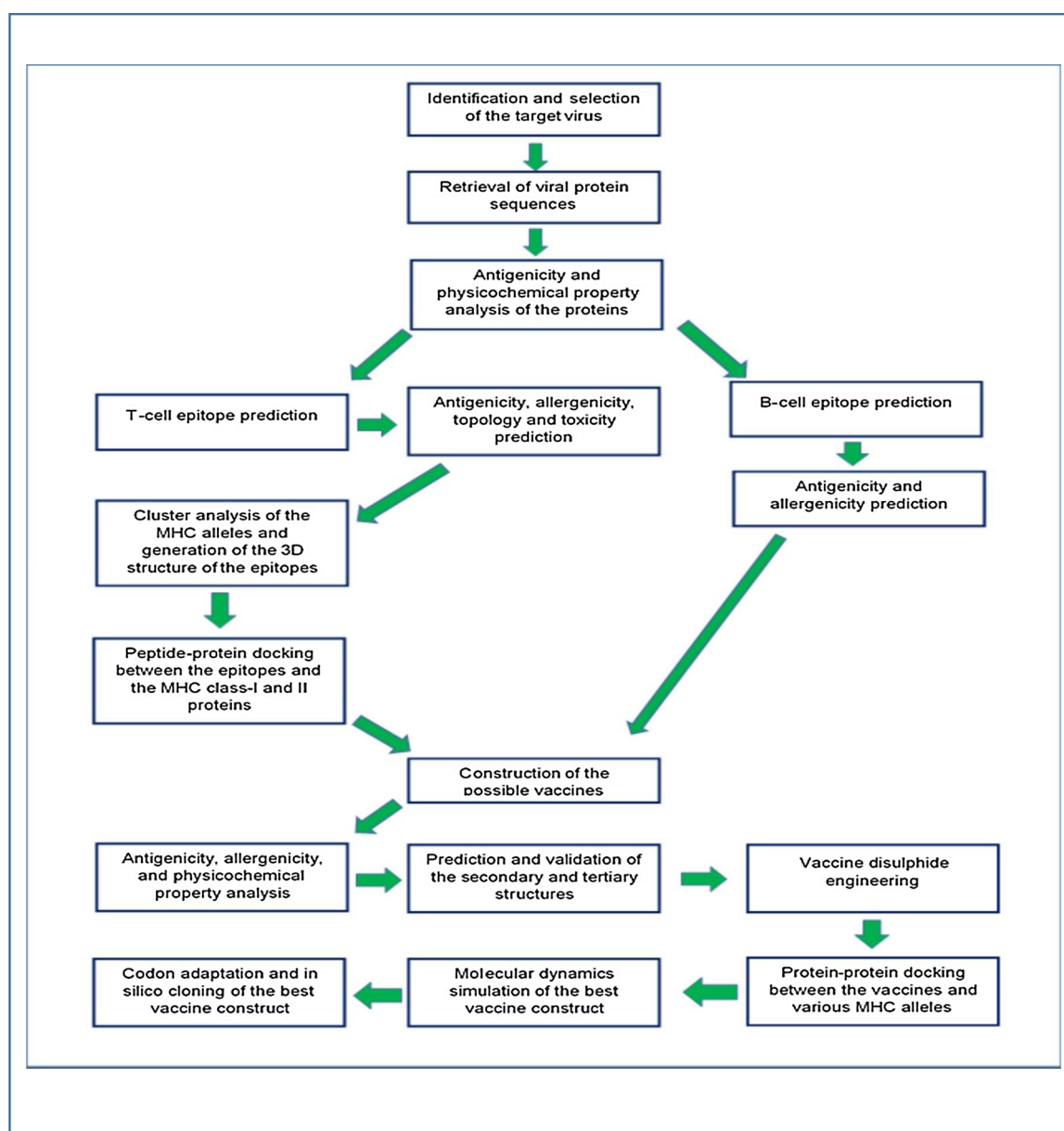


Fig. 1. Step-by-step strategies employed in the overall vaccine designing study.

**Table 1**  
Table lists the proteins of SARS-CoV-2 used in the study with their accession numbers.

Serial no.	Name of the protein	Accession no.
01	Nucleocapsid phosphoprotein	QHD43423.2
02	Membrane glycoprotein	QHD43419.1
03	ORF3a protein	QHD43417.1
04	Surface glycoprotein	QHD43416.1

the NCBI database in fasta format. **Table 1** lists the proteins sequences with their NCBI accession numbers.

**3.2. Antigenicity prediction and physicochemical property analysis of the protein sequences**

Two proteins: nucleocapsid phosphoprotein and surface glycoprotein, were identified as potent antigens and used in the next phases of the experiment (**Table 2**). The physicochemical property analysis was conducted for these two selected proteins. Nucleocapsid phosphoprotein had the highest predicted theoretical pI of 10.07, however, surface glycoprotein had the highest predicted extinction co-efficient of 148960 M<sup>-1</sup> cm<sup>-1</sup>. Both of them were found to have similar predicted half-life of 30 h. However, surface glycoprotein had the highest predicted aliphatic index and grand average of hydropathicity (GRAVY) values among the two proteins (**Table 3**).

**3.3. T-cell and B-cell epitope prediction and their antigenicity, allergenicity and topology determination**

The MHC class-I and MHC class-II epitopes were determined for potential vaccine construction. The IEDB (<https://www.iedb.org/>) server generated a good number of epitopes. The server contains experimental data on antibody and T-cell epitopes from studied conducted on humans, non-human primates and other animal species in the context of allergy, infectious disease, autoimmunity and transplantation. The server generates epitopes by analyzing these experimental data (Vita et al., 2018). However, based on the antigenicity scores, ten epitopes were selected from the top twenty epitopes because the epitopes generated almost similar AS and percentile scores. The percentile scores represent the predicted binding affinity and lower percentile scores correspond to higher binding affinity (Vita et al., 2018). Later, the epitopes with high antigenicity, non-allergenicity and non-toxicity were selected for vaccine construction. The B-cell epitopes were also selected based on their antigenicity, non-allergenicity and length (the sequences with more than 10 amino acids).

**Table 4** lists the potential T-cell epitopes of nucleocapsid phosphoprotein and **Table 5** lists the potential T-cell epitopes of surface glycoprotein. **Table 6** lists the predicted B-cell epitopes of the two proteins and **Table 7** lists the epitopes that followed the mentioned criteria and were selected for further analysis and vaccine construction.

**3.4. Cluster analysis of the MHC alleles**

The online tool MHCcluster 2.0 (<http://www.cbs.dtu.dk/services/MHCcluster/>), was used for the prediction or cluster analysis of the

**Table 2**  
The antigenicity determination of the selected proteins.

Name of the protein	Antigenicity (threshold = 0.4; tumor model)
Nucleocapsid phosphoprotein	Antigenic (0.709)
Membrane glycoprotein	Non-antigenic (0.166)
ORF3a protein	Non-antigenic (0.372)
Surface glycoprotein	Antigenic (0.534)

**Table 3**  
The physicochemical property analysis of the selected viral proteins.

Name of the protein sequence	Total amino acids	Molecular weight	Theoretical pI	Ext. coefficient (in M <sup>-1</sup> cm <sup>-1</sup> )	Est. half-life (in mammalian cell)	Aliphatic index	Grand average of hydropathicity (GRAVY)
Nucleocapsid phosphoprotein	419	45625.70	10.07	43890	30 h	52.53	- 0.971
Surface glycoprotein	1273	141178.47	6.24	148960	30 h	84.67	- 0.079

**Table 4**

MHC class-I and MHC class-II epitope prediction and topology, antigenicity, allergenicity and toxicity analysis of the epitopes of nucleocapsid phosphoprotein. AS; Antigenic Score.

MHC class	Epitope	Start	End	Topology	AS	Percentile scores	Antigenicity (tumor model, threshold = 0.4)	Allergenicity	Toxicity	
MHC class-I	AGLPYGANK	119	127	Outside	0.547	0.28	Antigenic	Non-allergenic	Non-toxic	
	KTFPPTEPK	361	369	Outside	0.967	0.01	Non-antigenic	Non-allergenic	Non-toxic	
	AADLDDFSK	397	405	Outside	0.235	0.96	Antigenic	Non-allergenic	Non-toxic	
	KSAAEASKK	249	257	Inside	0.670	0.17	Antigenic	Allergenic	Non-toxic	
	TQALPQRQK	379	387	Inside	0.349	0.60	Non-antigenic	Allergenic	Non-toxic	
	SSRGTSPAR	201	209	Inside	0.166	1.40	Antigenic	Allergenic	Non-toxic	
	ASWFTALTQ	50	58	Inside	0.115	1.80	Antigenic	Allergenic	Non-toxic	
	QLESKMSGK	229	237	Inside	0.084	2.20	Antigenic	Non-allergenic	Non-toxic	
	KDQVILLNK	347	355	Inside	0.082	2.30	Antigenic	Allergenic	Non-toxic	
	GTTLPKGFY	164	172	Outside	0.169	1.30	Non-antigenic	Allergenic	Non-toxic	
	MHC class-II	QELIRQGTDYKH	289	300	Inside	2.90	3.60	Antigenic	Non-allergenic	Non-toxic
		ELIRQGTDYKHW	290	301	Inside	2.90	3.60	Antigenic	Allergenic	Non-toxic
		DQELIRQGTDYK	288	299	Inside	2.90	3.60	Antigenic	Allergenic	Non-toxic
		SRIGMEVTPSGT	318	329	Inside	2.60	4.80	Non-antigenic	Non-allergenic	Non-toxic
LIRQGTDYKHWP		291	302	Inside	2.90	3.60	Antigenic	Non-allergenic	Non-toxic	
RLNQLESKMSGK		226	237	Inside	2.00	8.10	Antigenic	Non-allergenic	Non-toxic	
WFTALTQHGKED		52	63	Inside	1.70	11.0	Antigenic	Allergenic	Non-toxic	
LNQLESKMSGKG		227	238	Outside	2.00	8.10	Antigenic	Non-allergenic	Non-toxic	
LDRLNQLESKMS		224	235	Inside	2.00	8.10	Antigenic	Non-allergenic	Non-toxic	
WFTALTQHG		49	60	Outside	1.70	11.0	Antigenic	Allergenic	Non-toxic	

**Table 5**

MHC class-I and MHC Class-II epitope prediction and topology, antigenicity, allergenicity and toxicity analysis of the epitopes of surface glycoprotein. AS; Antigenic Score.

MHC class	Epitope	Start	End	Topology	AS	Percentile scores	Antigenicity (tumor model, threshold = 0.4)	Allergenicity	Toxicity	
MHC class-I	GVYFASTEK	89	97	Inside	0.938	0.01	Non-antigenic	Non-allergenic	Non-toxic	
	ASANLAATK	1020	1028	Inside	0.911	0.01	Non-antigenic	Allergenic	Non-toxic	
	SVLNDILSR	975	983	Inside	0.849	0.04	Antigenic	Non-allergenic	Non-toxic	
	GVLTESNKK	550	558	Inside	0.731	0.12	Antigenic	Non-allergenic	Non-toxic	
	SSTASALGK	939	947	Outside	0.779	0.09	Antigenic	Allergenic	Non-toxic	
	GTHWVFTQR	1099	1107	Inside	0.776	0.09	Non-antigenic	Allergenic	Non-toxic	
	EILPVSMTK	725	733	Inside	0.773	0.09	Non-antigen	Allergen	Non-toxic	
	ALDPLSETK	292	300	Outside	0.679	0.16	Antigenic	Allergenic	Non-toxic	
	RLFRKSNLK	454	462	Inside	0.677	0.16	Antigenic	Non-allergenic	Non-toxic	
	QIAPGQTGK	409	417	Inside	0.674	0.16	Antigenic	Non-allergenic	Non-toxic	
	MHC class-II	FLGVYYHKNNKS	140	151	Inside	4.40	0.45	Non-antigenic	Allergenic	Non-toxic
		TSNFRVQPTESI	315	326	Inside	5.30	0.08	Antigenic	Non-allergenic	Non-toxic
		VYYHKNNKSWME	143	154	Inside	4.40	0.45	Non-antigenic	Allergenic	Non-toxic
NFRVQPTESIVR		317	328	Inside	5.30	0.08	Antigenic	Allergenic	Non-toxic	
GVFVSNQTHWV		1093	1104	Outside	4.10	0.78	Non-antigenic	Allergenic	Non-toxic	
SNFRVQPTESIV		316	327	Inside	5.30	0.08	Antigenic	Non-allergenic	Non-toxic	
LLIVNATNVVI		117	128	Inside	4.30	0.58	Antigenic	Non-allergenic	Non-toxic	
EGVFVSNQTHWF		1092	1103	Outside	4.10	0.78	Non-antigenic	Allergenic	Non-toxic	
VFVSNQTHWVFT		1094	1105	Outside	4.10	0.78	Non-antigenic	Non-allergenic	Non-toxic	
IVNATNVVIKV		119	130	Inside	4.30	0.58	Antigenic	Allergenic	Non-toxic	

**Table 6**

B-cell epitope prediction and antigenicity, allergenicity analysis of the epitopes of nucleocapsid phosphoprotein and surface glycoprotein.

Nucleocapsid phosphoprotein			Surface glycoprotein		
Epitope	Antigenicity (tumor model, threshold = 0.4)	Allergenicity	Epitope	Antigenicity (tumor model, threshold = 0.4)	Allergenicity
MSDNGPQNQRNAPRITFGGSPSDSTGNSQNGERSGARSQRRPQGLPNNTAS	Antigenic	Non-allergenic	RTQLPPAYTNS	Non-antigenic	Allergenic
RIRGGDGKMKDL	Antigenic	Non-allergenic	LTPGDSSSGWTAG	Antigenic	Non-allergenic
TGPEAGLPYGANK	Antigenic	Non-allergenic	VRQIAPGQTGKIAD	Antigenic	Non-allergenic
GTTLPKGFYAEGRGGSQASSRSSRSRNSRNSTPGSSRGTSPARMAGNGGD	Antigenic	Non-allergenic	SGTNGTKRFDN	Antigenic	Allergenic
QHGKEDLKFRPGQGVPIINTSSPDDQIG	Non-antigenic	Non-allergenic	YQAGSTPCNGV	Antigenic	Non-allergenic
SKMSGKGQQQQTVTTKSAEASKKPRQKRTATKAYN	Antigenic	Non-allergenic	QTQTNSPRRARSV	Antigenic	Non-allergenic
KTFPPTEPKDKKKKADETQALPQRQKQKQ	Antigenic	Non-allergenic	ILPDPSKPSKRS	Antigenic	Non-allergenic
AFGRRGPEQTQGNFG	Non-antigenic	Allergenic	YGFQPTNGVGYQ	Non-antigenic	Allergenic
-	-	-	RDIADTTDAVRDPQ	Antigenic	Allergenic
-	-	-	VYDPLQPELDSF	Antigenic	Allergenic
-	-	-	KNHTSPDVDLG	Non-antigenic	Non-allergenic

**Table 7**

List of the epitopes that followed the selection criteria (high antigenicity, non-allergenicity and non-toxicity) and selected for vaccine construction.

Name of the proteins	MHC class-I epitopes	MHC class-II epitopes	B-cell epitopes
Nucleocapsid phosphoprotein	AGLPYGANK	QELIRQGTDYKH	MSDNGPQNQRNAPRITFGGSPDSTGNSQNGERSGARSKQRRPQGLPNNTAS
	AADLDDFSK	LIRQGTDYKHWP	RIRGGDGKMKDL
	QLESKMSGK	RLNQLESKMSGK	TGPEAGLPYGANK
	-	LNQLESKMSGK	GTTLPKGFYAEGSRGGSQASSRSSRSRNRSSRSTPGSSRGTSPARMAGNGGD
	-	LDRLNQLESKMS	SKMSGKGOQQGQTVTKKSAEASKPRQKRTATKAYN
Surface glycoprotein	SVLNDILSR	TSNFRVQPTESI	KTFPPTEPKDKKKKKADEQALPQRQKKQQ
	GVLTESNKK	SNFRVQPTESIV	LTPGDSSSGWTAG
	RLFRKSNLK	LLIVNNATNVVI	VRQIAPGQTGKIAD
	QIAPGQTGK	-	YQAGSTPCNGV
	-	-	QTQTNSPRRRSV
	-	-	ILPDPSPKPSKRS

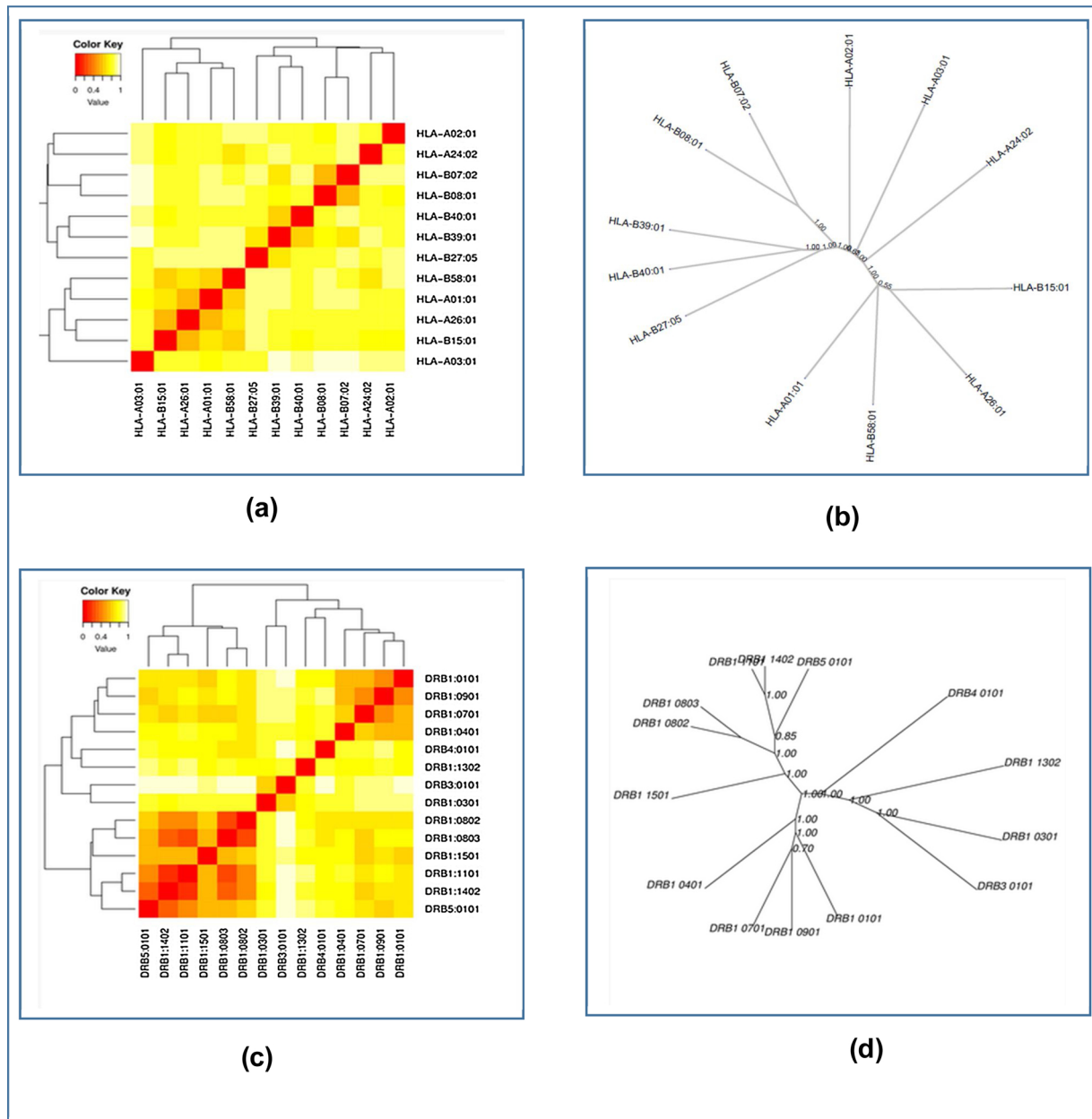


**Fig. 2.** The results of the MHC cluster analysis. Here, (a) is the heat map of MHC class-I cluster analysis, (b) is the tree map of MHC class-I cluster analysis, (c) is the heat map of MHC class-II cluster analysis, (d) is the tree map of MHC class-II cluster analysis.

**Table 8**  
Results of molecular docking analysis of the selected epitopes.

Name of the protein	Epitope	MHC allele	Global energy	Hydrogen bond energy	Epitope	MHC allele	Global energy	Hydrogen bond energy
Nucleocapsid phosphoprotein	AGLPYGANK	HLA-A*11-01	-38.28	-1.53	QELIRQGTDYKH	HLA DRB1*04-01	14.62	-1.09
	AADLDDFSK	allele (PDB ID: 5WJL)	-15.60	-2.69	LIRQGTDYKHWP	(PDB ID: 5JLZ)	-16.44	-1.66
	QLESKMSGK		-53.28	-4.32	RLNQLESKMSGK		-12.34	-3.41
	-		-	-	LNQLESKMSGKG		14.37	-9.20
Surface glycoprotein	-		-	-	LDRLNQLESKMS		-1.35	0.00
	SVLNDILSR		-27.72	-3.74	TSNFRVQPTESI		-2.28	0.00
	GVLTESNKK		-34.60	-3.64	SNFRVQPTESIV		1.82	0.00
	RLFRKSNLK		-27.48	-4.77	LLIVNNATNVVI		1.38	0.00
	QIAPGQTGK		-26.86	-0.89	-		-	-

possible MHC class-I and MHC class-II alleles that may interact with the selected epitopes during the immune responses. The tool illustrates the relationship of the clusters of the alleles in phylogenetic manner (Thomsen et al., 2013). Fig. 2 depicts the results of the cluster analysis where the red zone indicates strong interaction and the yellow zone corresponds to weaker interaction.

### 3.5. Generation of the 3D structures of the epitopes and peptide-protein docking

After 3D structure prediction of the selected epitopes, the peptide-protein docking was conducted to find out, whether all the epitopes had the ability to bind with the MHC class-I as well as MHC class-II molecules or not. The HLA-A\*11-01 allele (PDB ID: 5WJL) was used as the receptor for docking with the MHC class-I epitopes and HLA-DRB1\*04-01 (PDB ID: 5JLZ) was used as the receptor for docking with the MHC class-II epitopes. Among the MHC class-I epitopes of nucleocapsid phosphoprotein, QLESKMSGK showed the best result with the lowest global energy of -53.28. Among the MHC class-II epitopes of nucleocapsid phosphoprotein, LIRQGTDYKHWP generated the lowest and best global energy score of -16.44. GVLTESNKK generated the best global energy score of -34.60 of the MHC class-I epitopes of surface glycoprotein. And among the MHC class-II epitopes of surface glycoprotein,

TSNFRVQPTESI generated the best global energy score of -2.28 (Table 8 & Fig. 3).

### 3.6. Vaccine construction

After successful docking, three vaccines were constructed using the selected epitopes which are supposed to be directed to fight against the SARS-CoV-2. To construct the vaccines, three different adjuvants were used *i.e.*, beta defensin, L7/L12 ribosomal protein and HABA protein and different linkers *i.e.*, EAAAK, GGGs, GPGPG and KK linkers were used at their appropriate positions. PADRE sequence is an important sequence which was used in vaccine construction. It has the capability to increase the potency of the vaccines with minimal toxicity. Moreover, PADRE sequence also improve the CTL response, thus ensuring potent immune response (Wu et al., 2010). The newly constructed vaccines were designated as: CV-1, CV-2 and CV-3 (Table 9).

### 3.7. Antigenicity, allergenicity and physicochemical property analysis of the vaccine constructs

The results of the antigenicity, allergenicity and physicochemical property analysis are listed in Table 10. All the three vaccine constructs were found to be antigenic as well as non-allergenic. CV-3 had the

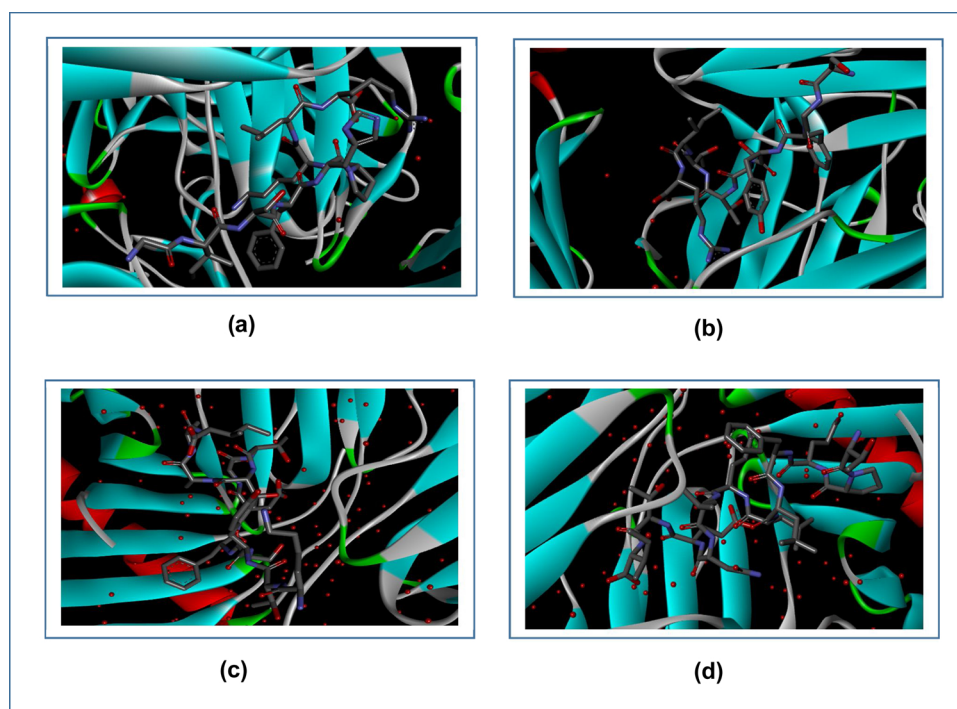


**Fig. 3.** The best poses of predicted interactions between the selected epitopes from the two proteins and their respective receptors. Here, (a) is the interaction between QLESKMSGK and MHC class-I, (b) is the interaction between GVLTESNKK and MHC class-I, (c) is the interaction between LIRQGTDYKHWP and MHC class-II, (d) is the interaction between TSNFRVQPTESI and MHC class-II. The interactions were visualized by Discovery Studio Visualizer.

**Table 9**

The three constructed SARS-CoV-2 vaccine constructs. In the vaccine sequences, the linkers are bolded for easy visualization.

Name of the vaccines	Vaccine constructs	Number of amino acids
Coronavirus vaccine-1 (CV-1)	EAAAKGIINTLQKYICRVRRGRCVAVLSCLPKKEEIQIGKCSRGRKCCRKKEAAAKAKFVAAWTLKAAAGGGSAGL- PYGANKGGSAADLDDFSKGGGSQLESKMSGKGGSSVLDILSRGGGSGVL- TESNKKGGGSRFRKSNLKGGSQIAPGQTGKGGPGPQELIRQGTDYKHGPGPGLIRQGT- DYKHWPGGPGRNLQLESKMSGKGGPGLNLQLESKMSGKGGPGLDRLNLQLESKMSGPPTSNSFRVQPT- SIGPGPGSNFRVQPTESIVGPGPGLLVNATNVVIKMSDNGPQNQRNAPRITFGGSDSTGNSQNGERS- GARSKQRRPQGLPNNTASKKRIRGGDGKMKDLKKTGPEAGLPYGANKKKGTTLPKGFYAEGRSGGS- QASSRSSSRNRSRSTPGSSRGTSARMAGNGGDKKSKMSGKGGQQGGQVTVTKSAEASKKPRQKRTAT- KAYNKKKTFPPEPKKDKKKKADETQALPQRQKQKQKLTGPDSSSGWTAGKKVQRQIAPGQTGKIADKKY- QAGSTPCNGVKKQTQTNSPRRARSVKKILPDPSPKSRKSKAKFVAAWTLKAAAGGGS	596
Coronavirus vaccine-2 (CV-2)	EAAAKMAKSTDELLDAFKEMTLELSDVFKFEETFEVTAAPVAVAAAGAAPAGAAVEAAEEQSEFDVI- LEAAGDKKIGVIVREIVSGLGLKEAKDLVDGAPKPLEKVAKEAADEAKAKLEAAGATVTVTKAAAKAF- VAAWTLKAAAGGGSAGLPYGANKGGSAADLDDFSKGGGSQLESKMSGKGGSSVLDILSRGGGSGVL- TESNKKGGGSRFRKSNLKGGSQIAPGQTGKGGPGPQELIRQGTDYKHGPGPGLIRQGT- DYKHWPGGPGRNLQLESKMSGKGGPGLNLQLESKMSGKGGPGLDRLNLQLESKMSGPPTSNSFRVQPT- SIGPGPGSNFRVQPTESIVGPGPGLLVNATNVVIGPGMSDNGPQNQRNAPRITFGGSDSTGNSQNGERS- GARSKQRRPQGLPNNTASKKRIRGGDGKMKDLKKTGPEAGLPYGANKKKGTTLPKGFYAEGRSGGS- QASSRSSSRNRSRSTPGSSRGTSARMAGNGGDKKSKMSGKGGQQGGQVTVTKSAEASKKPRQKRTAT- KAYNKKKTFPPEPKKDKKKKADETQALPQRQKQKQKLTGPDSSSGWTAGKKVQRQIAPGQTGKIADKKY- QAGSTPCNGVKKQTQTNSPRRARSVKKILPDPSPKSRKSKAKFVAAWTLKAAAGGGS	681
Coronavirus vaccine-3 (CV-3)	EAAAKMAENPIDLAPLALGAADLALATVNDLIANLRERAEETRAETRTRVEERRARLTKFQEDLPEQ- FIELRDKFTTEELRKAEGYLEAATNRYNELVERGEAALQRLRSQTAFEDASARAEGYVDQAVELTQEALGTVASQ- TRAVGERAAKLVGIELEAAAKAFVAAWTLKAAAGGGSAGLPYGANKGGSAADLDDFSKGGGSQ- LESKMSGKGGSSVLDILSRGGGSGVLTESNKKGGGSRFRKSNLKGGSQIAPGQTGKGGPGPQELIRQGT- DYKHGPGPGLIRQGTDYKHWPGGPGRNLQLESKMSGKGGPGLNLQLESKMSGKGGPGLDRLNLQ- LESKMSGPPTSNSFRVQPTESIVGPGPGLLVNATNVVIKMSDNGPQNQRNAPRITFGGSDSTGNSQNGERS- GARSKQRRPQGLPNNTASKKRIRGGDGKMKDLKKTGPEAGLPY- GANKKKGTTLPKGFYAEGRSGGSQASSRSSSRNRSRSTPGSSRGTSARM- MAGNGGDKKSKMSGKGGQQGGQVTVTKSAEASKKPRQKRTATKAYNKKKTFPPEPKKDKKKKADET- QALPQRQKQKQKLTGPDSSSGWTAGKKVQRQIAPGQTGKIADKKYQAGSTPCNGVKKQTQTNSPRRARSVK- KILPDPSPKSRKSKAKFVAAWTLKAAAGGGS	710

highest predicted molecular weight, extinction co-efficient and aliphatic index of 74505.61, 36900 M<sup>-1</sup> cm<sup>-1</sup> and 54.97 respectively. All of them had predicted *in vivo* half-life of 1 h and CV-2 was found to possess the highest GRAVY value of -0.830 among the three vaccines.

### 3.8. Secondary and tertiary structure prediction of the vaccine constructs

From the secondary structure analysis, it was determined that, the CV-1 vaccine construct had the highest percentage of the amino acids (67.1 %) in the coil formation as well as the highest percentage of amino acids (8%) in the beta-strand formation. However, CV-3 had the highest percentage of 37.8 % of amino acids in the alpha-helix formation (Fig. 4 and Table 11). Again, both CV-1 and CV-2 vaccines had 02 domains, whereas, CV-3 had only one domain. CV-2 had the lowest p-value of 6.35e-05. The p-value represents the relative quality of a protein model. The smaller p-value refers to higher quality of the protein model and vice-versa. Therefore, CV-2 showed the best performance in the 3D structure generation experiment. Moreover, three different templates were used for generating 3D structures of the three different vaccines. The RaptorX server used these templates for generating the 3D structures of the query vaccine constructs (Källberg et al., 2012). The results of the 3D structure analysis are listed in Table 12 and illustrated in Fig. 5.

### 3.9. 3D structure refinement and validation

The three vaccine constructs were refined and then validated in the 3D structure refinement and validation step. The PROCHECK server (<https://servicesn.mbi.ucla.edu/PROCHECK/>) divides the Ramachandran plot into four regions: the most favored region (represented by red color), the additional allowed region (represented by yellow color), the generously allowed region (represented by light yellow color) and the disallowed region (represented by white color).

According to the server, a valid protein (the best quality protein) should have over 90 % of its amino acids in the most favored region. The additional allowed region and generously allowed region might also contain some percentage of the amino acids of the protein. However, no amino acid should reside within the disallowed region (Sateesh et al., 2010; Laskowski et al., 1993; Zobayer, 2018).

The 3D protein structures generated in the previous step were refined for further analysis and validation. The refined structures were validated with the aid of the Ramachandran Plots. The analysis showed that CV-1 vaccine had excellent percentage of 94.3 % of the amino acids in the most favored region, 4.4 % of the amino acids in the additional allowed regions, 0.0 % of the amino acids in the generously allowed regions and 1.3 % of the amino acids in the disallowed regions. The CV-2 vaccine had 90.0 % of the amino acids in the most favored regions, 8.3 % of the amino acids in the additional allowed regions, 0.6 % of the amino acids in the generously allowed regions and 1.1 % of the amino acids in the disallowed regions. The CV-3 vaccine showed the worst result with 77.4 % of the amino acids in the most favored regions, 20.9 % of the amino acids in the additional allowed regions, 1.4 % of the amino acids in the generously allowed regions and 0.3 % of the amino acids in the disallowed regions (Fig. 6).

### 3.10. Vaccine protein disulfide engineering

In protein disulfide engineering, disulfide bonds were generated within the 3D structures of the vaccine constructs. In the experiment, the amino acid pairs that had bond energy value less than 2.00 kcal/mol, were selected. Since about 90 % of the native disulfide bonds in proteins have energy value of less than 2.2 kcal/mol, the bond energy value of 2.00 kcal/mol was selected as the cut-off value for the experiment for better prediction (Craig and Dombkowski, 2013). The CV-1 generated 10 amino acid pairs that had the capability to form disulfide bonds. However, only one pair was selected because they had the

**Table 10**  
The antigenicity, allergenicity and physicochemical property analysis of the vaccine constructs. MW; Molecular Weight.

Name of the vaccine constructs	Total amino acids	Antigenicity (tumor model, threshold = 0.4)	Allergenicity	MW	Theoretical pI	Ext. coefficient (in $M^{-1} \text{cm}^{-1}$ )	Est. half-life (in mammalian cell)	Aliphatic index	Grand average of hydropathicity (GRAVY)
CV-1	596	Antigenic	Non-allergenic	62038.16	10.69	35785	1 h	46.26	-1.041
CV-2	681	Antigenic	Non-allergenic	70317.45	10.23	32430	1 h	55.86	-0.830
CV-3	710	Antigenic	Non-allergenic	74505.61	10.31	36900	1 h	54.97	-0.941

bond energy, less than 2.00 kcal/mol: 276 Ser-311 Arg. Although, CV-2 and CV-3 generated 04 and 05 pairs of amino acids, respectively, that might form disulfide bonds but no pair of amino acids showed bond energy less than 2.00 Kcal/mol. The selected amino acid pairs of CV-1 formed the mutant version of the original vaccines (Fig. 7).

### 3.11. Protein-protein docking study

The protein-protein docking study was carried out to find out the best constructed COVID-19 vaccine. The vaccine construct with the best result in the molecular docking, was considered as the best vaccine construct. According to docking results, it was found that CV-1 was the best constructed vaccine. CV-1 showed the best and lowest scores in the docking as well as in the MM-GBSA study by HawkDock server. However, CV-2 showed the best binding affinity ( $\Delta G$  scores) with DRB3\*0202 (-18.9 kcal/mol) and DRB1\*0301 (-18.5 kcal/mol) when analyzed with ClusPro 2.0 and the PRODIGY tool of HADDOCK server. Moreover, when analyzed with PatchDock and FireDock servers, CV-3 showed best global energy scores with the MHC alleles *i.e.*, DRB5\*0101 (-10.70), DRB5\*0101 (-19.59), DRB1\*0101 (-17.46) and DRB3\*0101 (-12.32). Since CV-1 showed the best results in the protein-protein docking study with almost all the targets by all the servers and also with the TLR-8, it was considered as the best vaccine construct among the three constructed vaccines (Fig. 8 and Table 13). Later, the molecular dynamics simulation and in silico codon adaptation studies were conducted only on the CV-1 vaccine.

### 3.12. Molecular dynamics simulation study

The results of molecular dynamics simulation of CV-1-TLR-8 docked complex is illustrated in Fig. 9. Dynamic simulation of proteins gives easy determination of the stability and physical movements of their atoms and molecules (Chauhan et al., 2019). So, the simulation was carried out to determine the relative stability of the vaccine protein. The deformability graph of the complex illustrates the peaks representing the regions of the protein with moderate degree of deformability (Fig. 9b). The B-factor graph of the complex gives easy visualization and comparison between the NMA and the PDB field of the docked complex (Fig. 9c). The eigenvalue of the docked complex is depicted in Fig. 9d. CV-1 and TLR8 docked complex generated quite good eigenvalue of 3.817339e-06. The variance graph illustrates the individual variance by red colored bars and cumulative variance by green colored bars (Fig. 9e). Fig. 10f depicts the co-variance map of the complex, where red color represents the correlated motion between a pair of residues, uncorrelated motion is indicated by white color as well as the anti-correlated motion is marked by blue color. The elastic map of the complex refers to the connection between the atoms and darker gray regions indicate stiffer regions (Fig. 9g) (López-Blanco et al., 2014; López-Blanco et al., 2011; Kovacs et al., 2004).

### 3.13. Codon adaptation and in silico cloning study

Since the CV-1 protein had 596 amino acids, after reverse translation, the number nucleotides of the probable DNA sequence of CV-1 would be 1788. The codon adaptation index (CAI) value of 1.0 of CV-1 indicated that the DNA sequences contained higher proportion of the codons that should be used by the cellular machinery of the target organism *E. coli* strain K12 (codon bias). For this reason, the production of the CV-1 vaccine should be carried out efficiently (Solanki and Tiwari, 2018; Carbone et al., 2003). The GC content of the improved sequence was 51.34 % (Fig. 10). The predicted DNA sequence of CV-1 was inserted into the pET-19b vector plasmid between the SgrAI and SphI restriction sites and since the vaccine DNA sequence did not have restriction sites for SgrAI and SphI restriction enzymes, SgrAI and SphI restriction sites were conjugated at the N-terminal and C-terminal sites, respectively. The newly constructed vector is illustrated in Fig. 11.

4. Discussion

The current study was designed to construct possible vaccines against the SARS-CoV-2, which is the cause of the recent pandemic of the deadly viral disease, COVID-19 around the world. The pneumonia has already caused the death of thousands of people worldwide. For this reason, possible vaccines were predicted in this study to fight against this lethal virus. To carry out the vaccine construction, four candidate proteins of the virus were identified and selected from the NCBI database. Only highly antigenic sequences were selected for further analysis since the highly antigenic proteins can induce better immunogenic response (Demkowicz et al., 1992). Because the nucleocapsid phosphoprotein and surface glycoprotein were found to be antigenic, they were taken into consideration for vaccine construction.

The physicochemical property analysis was conducted for the two predicted antigenic proteins. The extinction coefficient can be defined as the amount of light that is absorbed by a particular compound at a certain wavelength. Surface glycoprotein had the highest predicted extinction co-efficient of 148960 M<sup>-1</sup> cm<sup>-1</sup>. The aliphatic index of a protein corresponds to the relative volume occupied by the aliphatic amino acids in the side chains of the protein, for example: alanine, valine etc. (Pace et al., 1995; Gill and Von Hippel, 1989; Ikai, 1980; Ullah et al., 2020b). Surface glycoprotein also had the highest predicted aliphatic index among the two proteins (84.67). Therefore, surface glycoprotein had greater amount of aliphatic amino acids in its side chain than the nucleocapsid phosphoprotein. The grand average of hydropathicity value (GRAVY) for a protein is calculated as the sum of hydropathy values of all the amino acids of the protein, divided by the

number of residues in its sequence. The negative GRAVY value represents hydrophilic characteristic and the positive GRAVY value represents hydrophobic characteristic of a compound (Kyte and Doolittle, 1982; Chang and Yang, 2013). Surface glycoprotein had the highest predicted GRAVY value of -0.079 among the two proteins. Since both proteins had the predicted negative GRAVY value, both of them were considered to be hydrophilic. Moreover, both of them had the predicted *in vivo* half-life of 30 h and nucleocapsid phosphoprotein had the highest theoretical pI of 10.07. Both the proteins showed quite good results in the physicochemical property analysis.

After the physicochemical property analysis of the protein sequences, the T-cell and B-cell epitope prediction was conducted. T-cell and B-cell are the two main types of cells that function in immunity. When an antigen is encountered in the body by the immune system, the antigen presenting cells or APC like macrophage, dendritic cell etc. present the antigen to the T-helper cell, through the MHC class-II molecules on their surface. The helper T-cell contains CD4+ molecule on its surface, for this reason, it is also known as CD4 + T-cell. On the other hand, the other type of T-cell, cytotoxic T-cell contains CD8+ molecule on its surface, for which, they are called CD8 + T-cell. MHC class-I molecules present antigens to cytotoxic T-lymphocytes. After activation by the antigen, the T-helper cell activates the B-cell, which starts to produce large amount of antibodies. Macrophage and CD8 + cytotoxic T cell are also activated by the T-helper cell that cause the final destruction of the target antigen (Goerdts and Orfanos, 1999; Tanchot and Rocha, 2003; Pavli et al., 1993; Arpin et al., 1995; Cano and Lopera, 2013). The possible T-cell and B-cell epitopes of the selected proteins were determined by the IEDB (<https://www.iedb.org/>)



Fig. 4. Results of the secondary structure prediction of the three vaccine constructs. Here, (a) is the CV-1 vaccine, (b) is the CV-2 vaccine, (c) is the CV-3 vaccine.

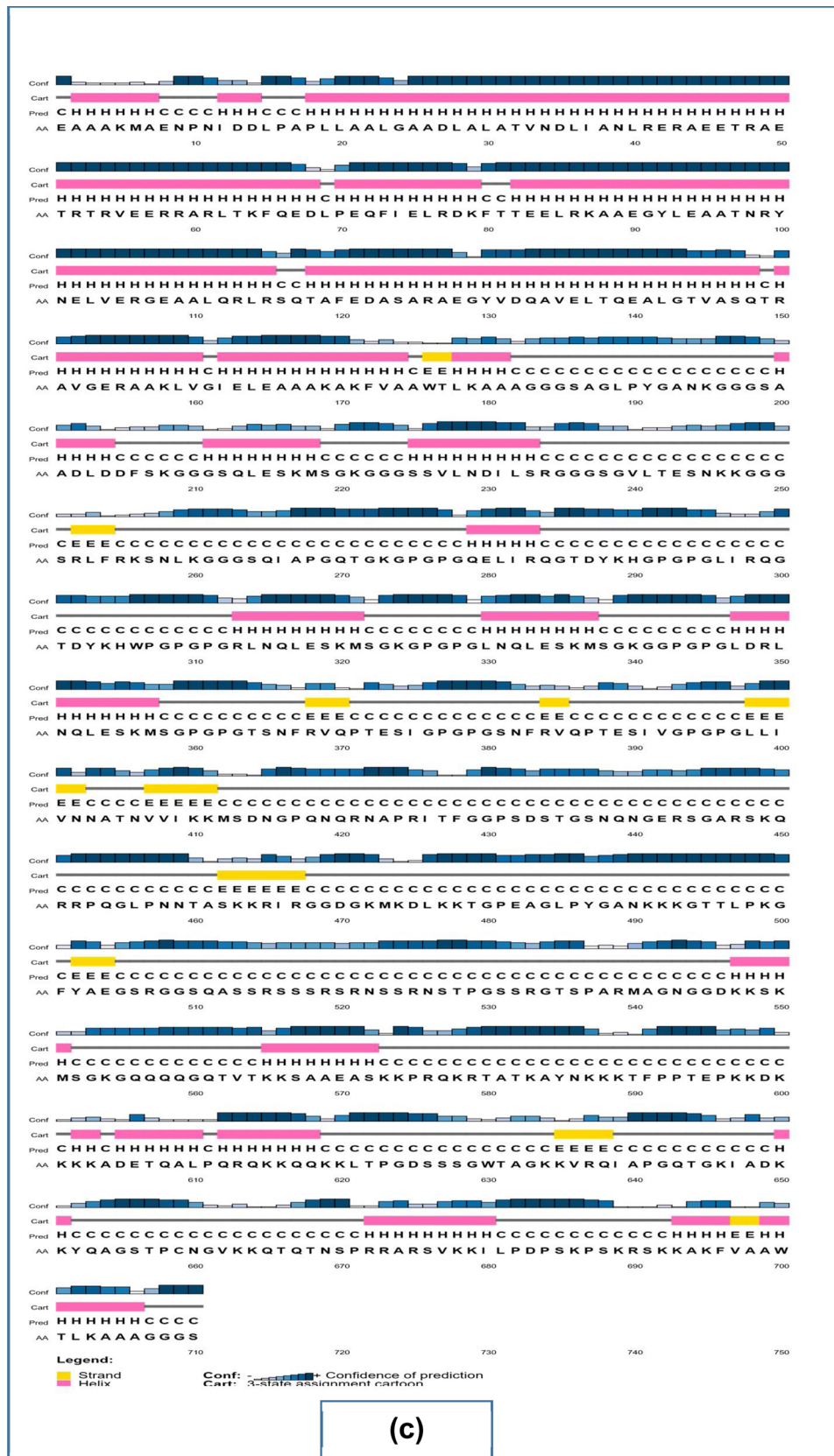


Fig. 4. (continued)

**Table 11**  
Results of the secondary structure analysis of the vaccine constructs.

Name of the vaccine	Alpha helix (percentage of amino acids)	Beta sheet (percentage of amino acids)	Coil structure (percentage of amino acids)
CV-1	25 %	8%	67.1 %
CV-2	31.6%	6.8 %	61.6 %
CV-3	37.8 %	5%	57.2 %

**Table 12**  
Results of the tertiary structure analysis of the vaccine constructs.

Name of the vaccine	Number of the domains	p-value	PDB Id of the est. matched template
CV-1	02	2.37e-04	1kj6A
CV-2	02	6.35e-05	1dd3A
CV-3	01	2.36e-04	6cfeA

server. The epitopes with high antigenicity, non-allergenicity and non-toxicity were selected to construct the vaccines. The B-cell epitopes (predicted by the server) that were more than ten amino acids long were taken into consideration and the antigenic and non-allergenic epitopes were selected for vaccine construction. However, most of the epitopes were found to be located within the cell membrane.

The cluster analysis of the MHC alleles which may interact with the

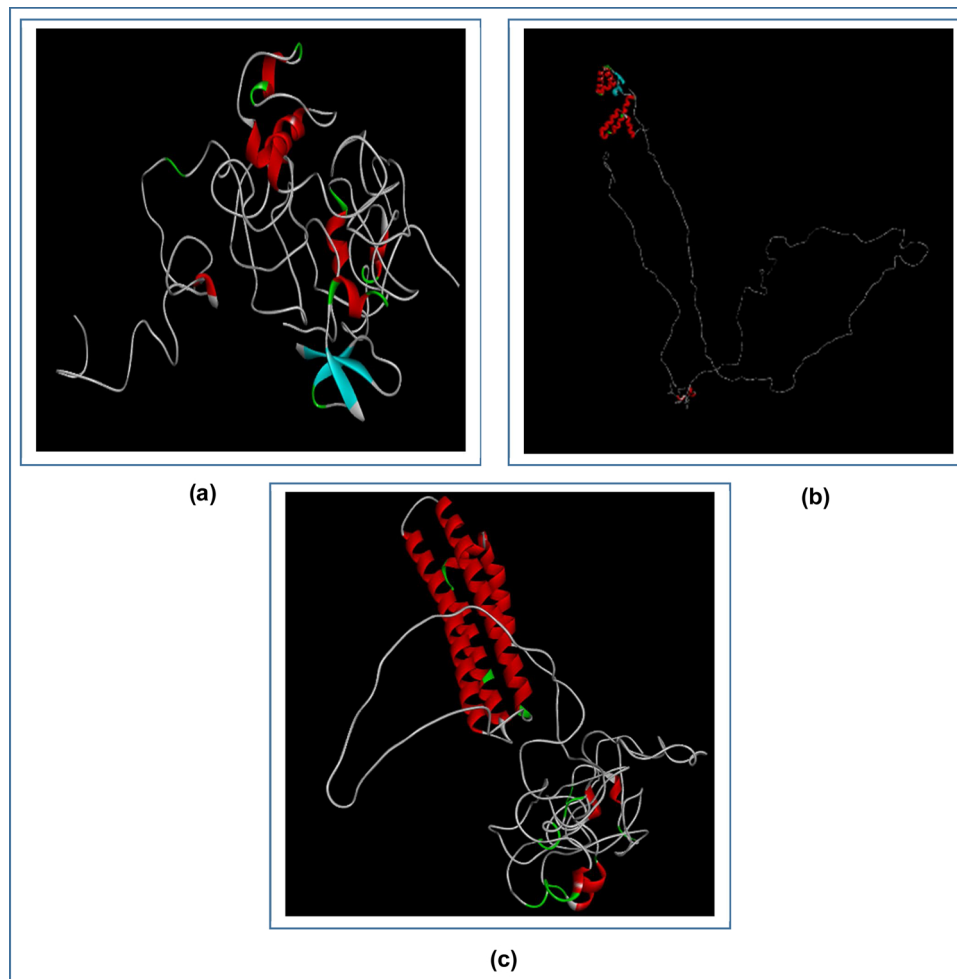


**Fig. 5.** 3D structures of the three predicted vaccine constructs. Here, (a) is CV-1, (b) is CV-2, (c) is CV-3.

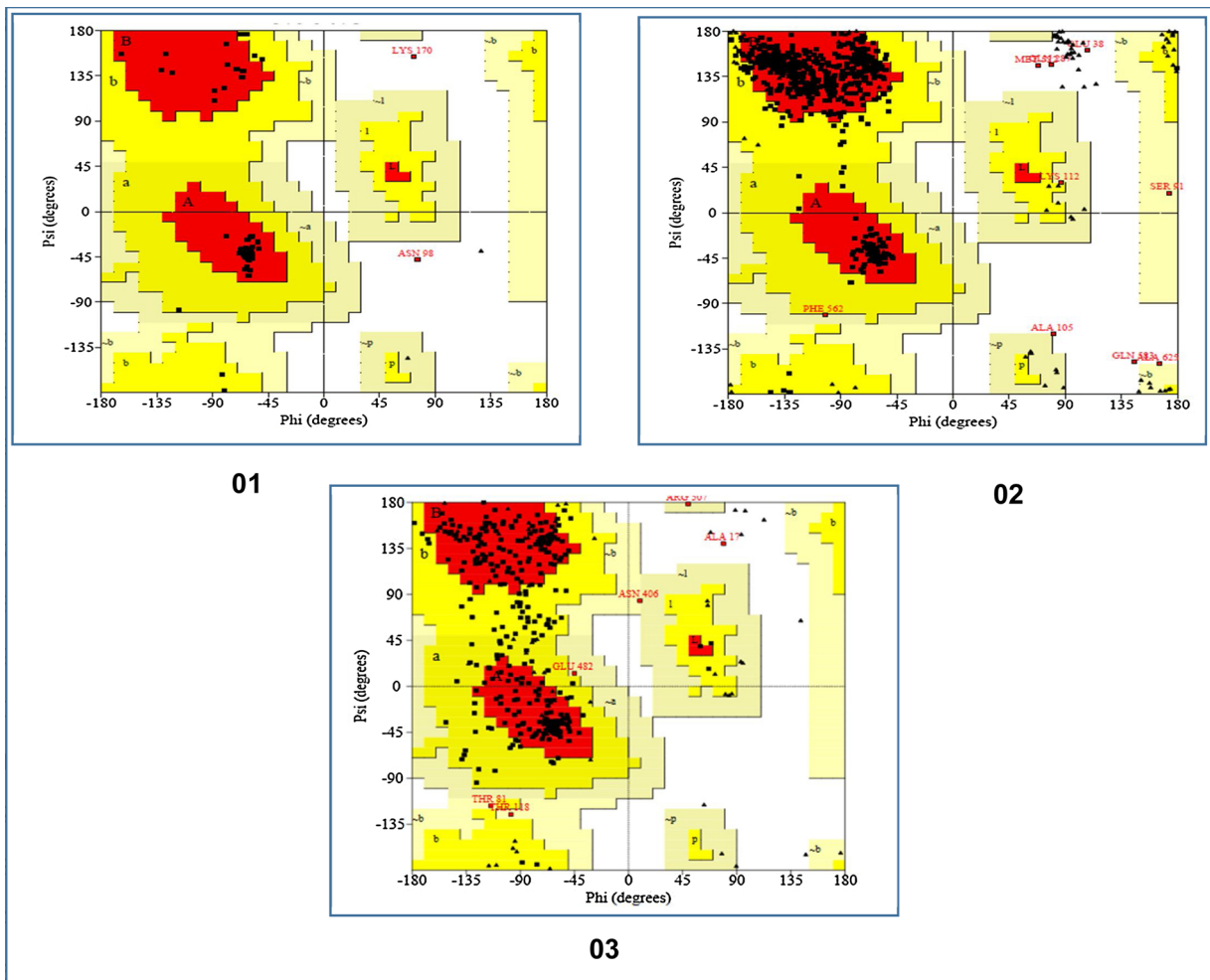


Fig. 6. The results of the Ramachandran plot analysis of the three coronavirus vaccine constructs. Here, 01. CV-1 vaccine, 02. CV-2 vaccine, 03. CV-3 vaccine.

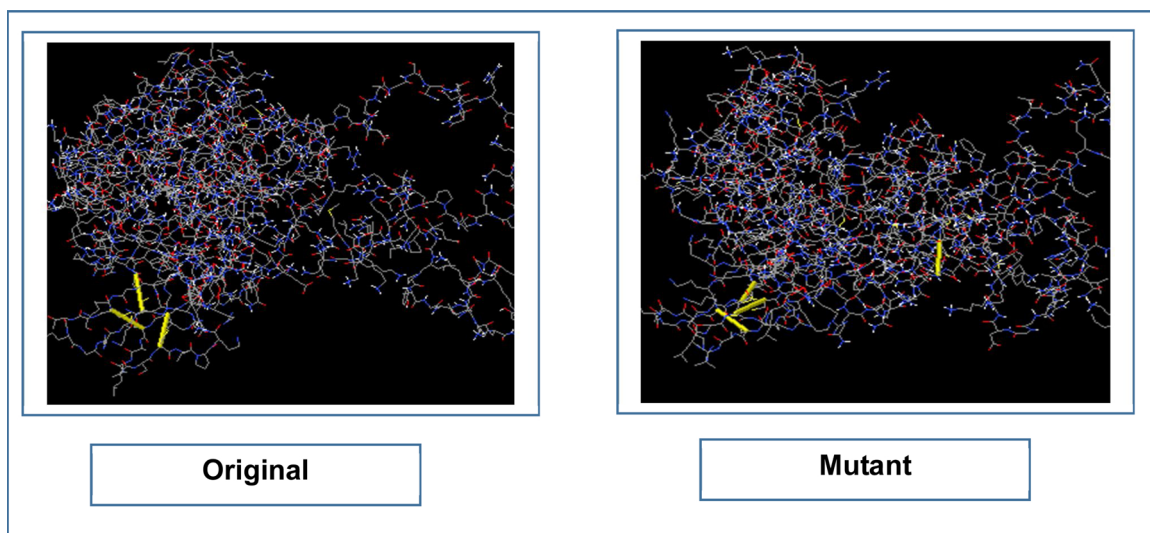
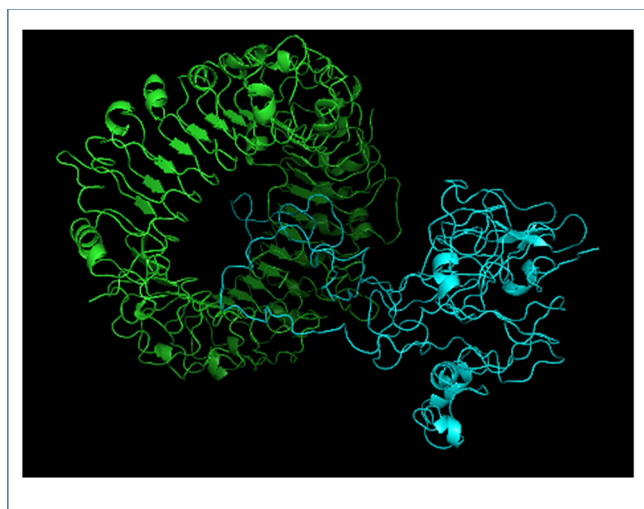


Fig. 7. The disulfide engineering of CV-1. The original form is illustrated in the left side and the mutant form is illustrated in the right side.



**Fig. 8.** The interaction between TLR-8 (in green color) and CV-1 vaccine construct (in light blue color). The interaction was visualized with PyMol.

**Table 13**

Results of the docking study of all the vaccine constructs.

Name of the vaccines	Name of the Targets	PDB IDs of the targets	Binding affinity, $\Delta G$ (kcal mol <sup>-1</sup> )	Global energy	HawkDock score (the lowest score)	MM-GBSA (binding free energy, in kcal mol <sup>-1</sup> )
CV-1	DRB3*0202	1A6A	-17.2	-4.22	-6436.60	-55.56
	DRB5*0101	1H15	-19.9	-4.92	-6669.84	-141.66
	DRB1*0101	2FSE	-19.1	4.31	-7297.17	-148.58
	DRB3*0101	2Q6W	-19.2	-7.20	-7581.70	-138.4
	DRB1*0401	2SEB	-21.4	-11.58	-6758.33	-98.56
	DRB1*0301	3C5J	-17.7	-9.09	-5201.43	-114.35
	TLR8	3W3M	-23.2	-23.12	-6514.36	-52.06
	DRB3*0202	1A6A	-18.9	-10.32	-3477.55	1.01
CV-2	DRB5*0101	1H15	-17.7	-10.46	-3761.37	-106.17
	DRB1*0101	2FSE	-16.9	1.58	-3531.12	-106.13
	DRB3*0101	2Q6W	-19.1	16.68	-3707.86	-90.89
	DRB1*0401	2SEB	-20.0	-10.01	-4766.17	-45.76
	DRB1*0301	3C5J	-18.5	-1.87	-3561.16	-18.72
	TLR8	3W3M	-21.1	-18.91	-2945.44	-54.79
	DRB3*0202	1A6A	-16.9	-10.70	-4023.68	-9.2
	DRB5*0101	1H15	-18.9	-19.59	-4556.87	-12.38
CV-3	DRB1*0101	2FSE	-17.1	-17.46	-4602.08	-10.54
	DRB3*0101	2Q6W	-18.4	-12.32	-4767.21	-27.71
	DRB1*0401	2SEB	-20.1	6.55	-3571.79	-8.74
	DRB1*0301	3C5J	-17.8	5.35	-4001.56	-12.38
	TLR8	3W3M	-22.8	-10.92	-5008.23	-19.83

selected epitopes during the immune response, showed quite good interaction with each other. Next the 3D structures of the selected epitopes were generated for peptide-protein docking study. The docking was performed to find out whether all the epitopes had the capability to bind with their respective MHC class-I and MHC class-II alleles or not. Since all the epitopes generated quite good docking scores, it can be

concluded that, all of them had the capability to bind with their respective targets and induce potential immune response. However, among the selected epitopes, QLESKMSGK, LIRQGTDYKHWP, GVLTE-SNKK and TSNFRVQPTESI generated the best docking scores.

After the successful docking study, the vaccine construction was performed. The linkers were used to connect the T-cell and B-cell epitopes among themselves and also with the adjuvant sequences as well as the PADRE sequence. The vaccines, with three different adjuvants, were constructed and designated as: CV-1, CV-2 and CV-3. Since all the three vaccines were found to be antigenic, they should be able to induce good immune response. Moreover, all of them were non-allergenic, so they should not be able to cause any allergenic reaction within the body as per *in silico* prediction. With the highest aliphatic index of 54.97, CV-3 had the highest predicted number of aliphatic amino acids in its side chains. The highest theoretical pI of CV-1 indicated that it requires high pH to reach the isoelectric point. Quite similar values of extinction coefficient were generated by the three vaccine constructs. These three vaccine constructs showed quite good and similar results in the physicochemical property analysis.

The secondary structure prediction of the vaccine constructs determined that CV-1 had the lowest number of amino acids in alpha-helix formation, with 25 % of the amino acids in the alpha-helix formation and 67.1 % of the amino acids in coil formation. For this reason, most of the amino acids of CV-1 vaccine were predicted to be in coil structure, which was also the highest percentage of amino acids in coil structure among the three vaccines. On the other hand, CV-3 had the highest amount of amino acids in the alpha-helix formation (37.8 %), according to the prediction of the study. However, all the three vaccine constructs had most of their amino acids in their coil structures. In the tertiary structure prediction, all the three vaccine constructs showed quite satisfactory results. Thereafter, in the tertiary structure refinement and validation, CV-1 vaccine construct generated the best result with 94.3 % of the amino acids in the most favored region and 4.4 % of the amino acids in the additional allowed regions. CV-2 also showed good result with 90.0 % of the amino acids in the most favoured region. In the disulfide bond engineering experiment, only CV-1 was found to follow the selection criteria for disulfide bond formation. With the lowest and best results generated by the MM-GBSA study, HawkDock server and ClusPro 2.0 server, CV-1 was considered as the best vaccine construct among the three vaccines. Therefore, CV-1 was selected for molecular dynamics simulation study, codon adaptation and *in silico* coding study. The molecular dynamics simulation study, conducted by the online tool iMODS (<http://imods.chaconlab.org/>) revealed that the TLR-8-CV-1 docked complex should be quite stable with a good eigenvalue of 3.817339e-06. The complex had less chance of deformation and for this reason, the complex should be quite stable in the biological environment. The Fig. 9f shows that a good number of amino acids were in the correlated motion that were marked by red color. Finally, codon adaptation and *in silico* cloning experiments were performed and with the predicted CAI value of 1.0, it could be concluded that the DNA sequence might contain very high amount of favorable codons that should be able to express the desired amino acids in the target microorganism, *E. coli* strain K12. The DNA sequence also had quite high and good amount of GC content of 51.34 %. Finally, the pET-19b vector, containing the CV-1 vaccine insert was constructed which should efficiently encode the vaccine protein in the *E. coli* cells.

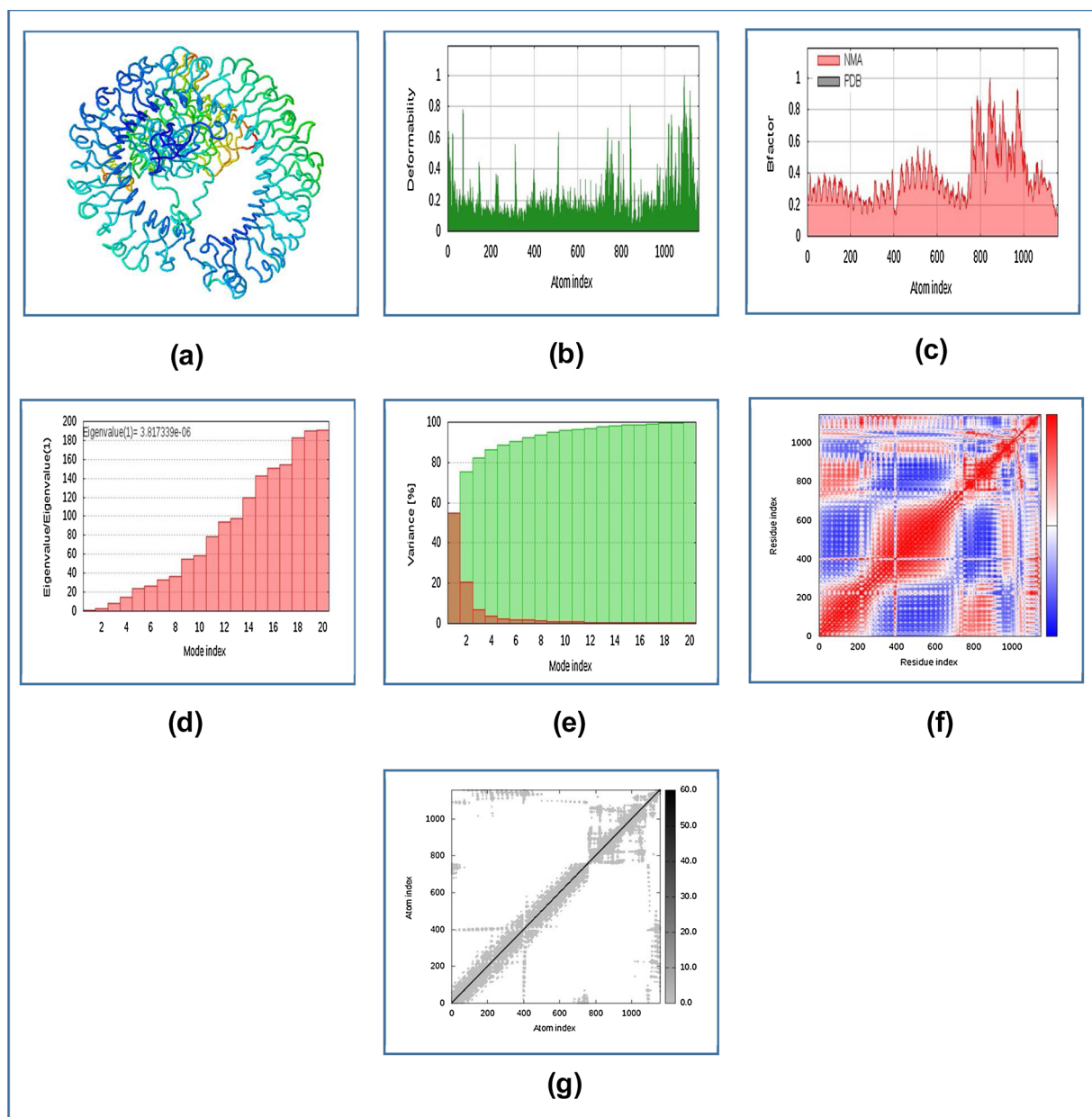


**Fig. 9.** The results of molecular dynamics simulation study of CV-1 and TLR-8 docked complex. Here, (a) NMA mobility, (b) deformability, (c) B-factor, (d) eigenvalues, (e) variance (red color indicates individual variances and green color indicates cumulative variances), (f) co-variance map (correlated (red), uncorrelated (white) or anti-correlated (blue) motions) and (g) elastic network (darker gray regions indicate more stiffer regions).

The vaccine development using genome based technologies provides scientists the opportunity to develop vaccines by optimizing the target antigens. Conventional vaccines, like the attenuated vaccines or the inactivated vaccines sometimes fail to provide potential immunity towards a target antigen. Moreover, the conventional approach of vaccine development has raised many safety concerns in the pre-clinical and clinical trials. The subunit vaccines like the vaccines predicted in the study could overcome such difficulties (Tameris et al., 2013;

Merten, 2002; Hasson et al., 2015; Kaufmann et al., 2014; Stratton et al., 2002). Finally, this study recommends CV-1 as the best vaccine to be an effective countermeasure based on the strategies employed in the study to be triggered against SARS-CoV-2 infection. However, further *in vivo* and *in vitro* experiments are suggested to strengthen the findings of this study.

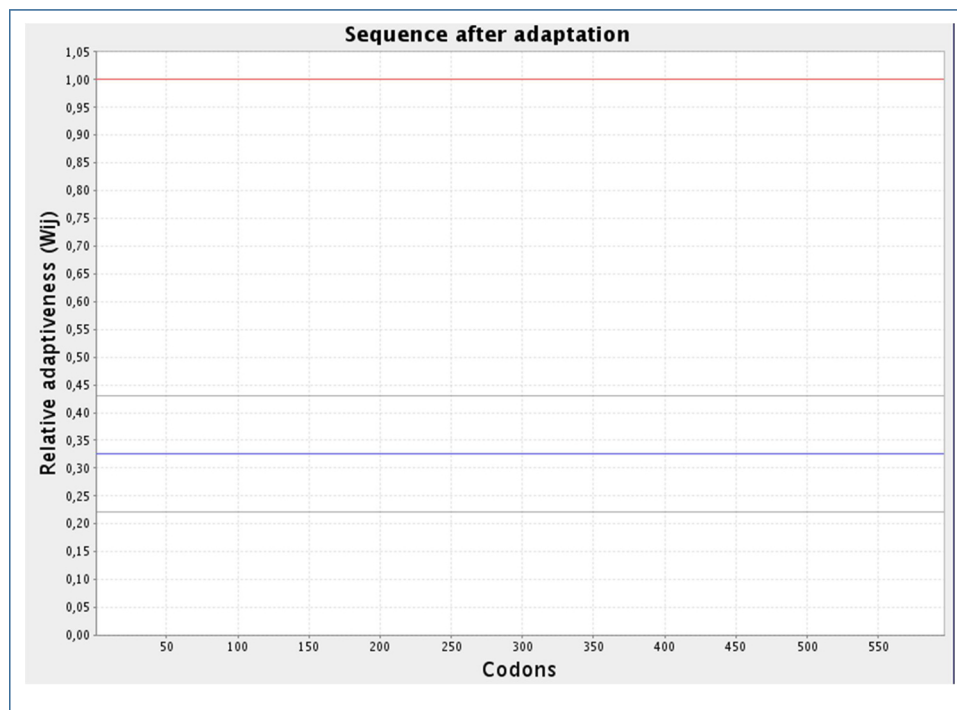


Fig. 10. The results of the codon adaptation study of the best constructed vaccine, CV-1.

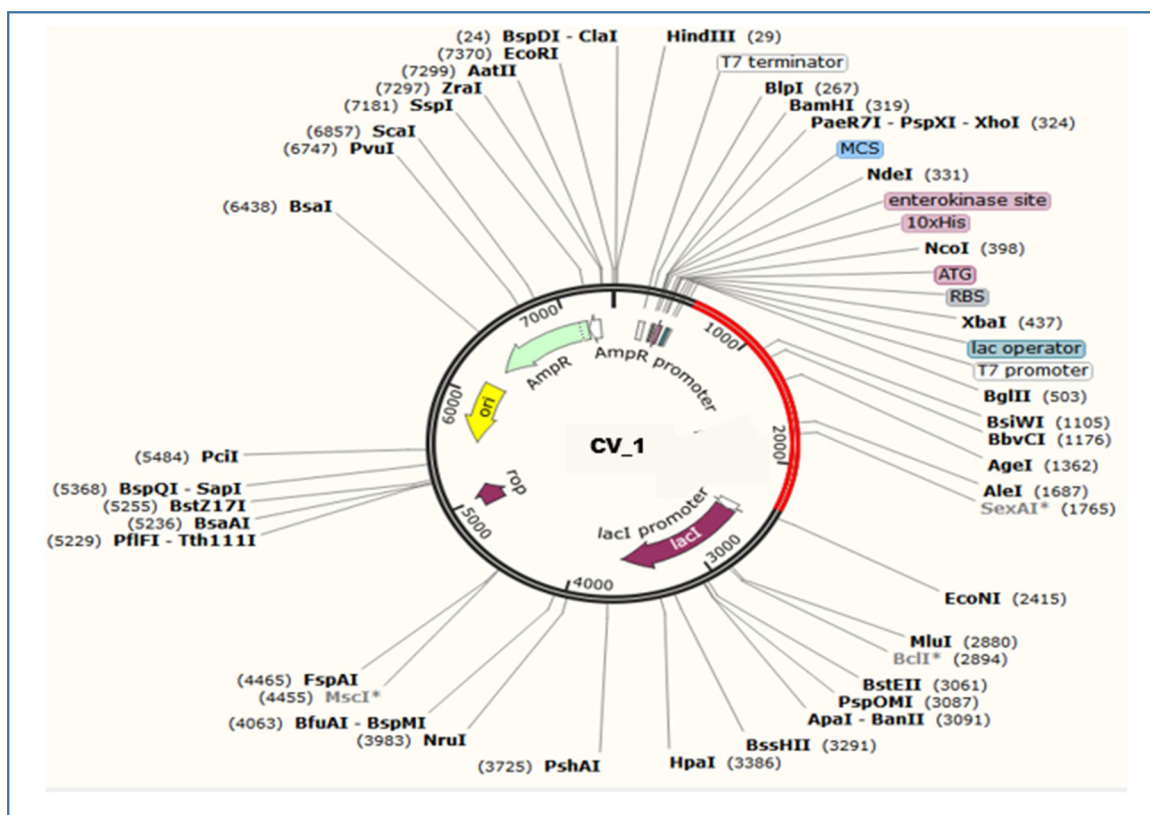


Fig. 11. Constructed pET-19b vector with the CV-1 insert (marked in red color). In the plasmid, the larger purple colored arrow represents the *lacI* gene (from 2500 bp to 3582 bp), the smaller purple colored arrow represents the *rop* gene (from 4896 bp to 5085 bp), yellow colored arrow represents the origin of replication (from 5517 bp to 6103 bp), the light green colored arrow represents the *AmpR* (ampicillin resistance) gene (from 6274 bp to 7134 bp), the white rectangle represents the T7 terminator (from 195 bp to 242 bp), the light blue colored arrow represents the multiple cloning site (from 301 bp to 317 bp) and the desired gene has been inserted (marked by red color) between the 485 bp and 2128 bp nucleotide. Various restriction enzyme sites are mentioned in the plasmid structure.

## 5. Conclusion

The SARS-CoV-2 has caused one of the deadliest pandemics in the recent times. Prevention of the newly emerging infection is very challenging as well as mandatory. The potentiality of *in silico* methods can be exploited to find desired solutions with fewer trials and errors and thus saving both time and cost of the scientists. In this study, potential subunit vaccines were designed against the SARS-CoV-2 using various methods of reverse vaccinology and immunoinformatics. To design the vaccines, the highly antigenic viral proteins as well as epitopes were used. Different types of computational studies on the suggested vaccine constructs revealed that these vaccines might confer good immunogenic response. Therefore, if satisfactory results are achieved in numerous *in vivo* and *in vitro* tests and trials, these suggested vaccine constructs might be used effectively for vaccination to prevent the SARS-CoV-2 infection and spreading. Therefore, our present study should help the scientists to develop potential vaccines and therapeutics against the SARS-CoV-2.

## Data availability statement

Authors made all the data generated during experiment and analysis available within the manuscript.

## Funding statement

Authors received no specific funding from any external sources.

## Declaration of Competing Interest

The authors declare that they have no known competing financial interests or personal relationships that could have appeared to influence the work reported in this paper.

## Acknowledgements

Authors acknowledge the members of Swift Integrity Computational Lab, Dhaka, Bangladesh, a virtual platform of young researchers for their support during the preparation of the manuscript.

## References

- Arpin, C., Dechanet, J., Van Kooten, C., Merville, P., Grouard, G., Briere, F., Banchereau, J., Liu, Y.J., 1995. Generation of memory B cells and plasma cells in vitro. *Science* 268, 720–722. <https://doi.org/10.1126/science.7537388>.
- Cano, R.L., Lopera, H.D., 2013. Introduction to T and B lymphocytes. *Autoimmunity: From Bench to Bedside*. El Rosario University Press.
- Carbone, A., Zinovyev, A., Képes, F., 2003. Codon adaptation index as a measure of dominating codon bias. *Bioinformatics* 19, 2005–2015. <https://doi.org/10.1093/bioinformatics/btg272>.
- Cavanagh, D., 1995. The coronavirus surface glycoprotein. *The Coronaviridae*. Springer, Boston, MA, pp. 73–113.
- Chang, K.Y., Yang, J.R., 2013. Analysis and prediction of highly effective antiviral peptides based on random forests. *PLoS One* 8 (8).
- Chang, C.K., Hou, M.H., Chang, C.K.F., Hsiao, C.D., Huang, T.H., 2014. The SARS coronavirus nucleocapsid protein-forms and functions. *Antiviral Res.* 1 (March (103)), 39–50.
- Chauhan, V., Rungta, T., Goyal, K., Singh, M.P., 2019. Designing a multi-epitope based vaccine to combat Kaposi Sarcoma utilizing immunoinformatics approach. *Sci. Rep.* 9, 1–5. <https://doi.org/10.1038/s41598-019-39299-8>.
- Chong, L.C., Khan, A.M., 2019. Vaccine Target Discovery. <https://doi.org/10.1016/b978-0-12-809633-8.20100-3>.
- Craig, D.B., Dombkowski, A.A., 2013. Disulfide by Design 2.0: a web-based tool for disulfide engineering in proteins. *BMC Bioinformatics* 14 (346). <https://doi.org/10.1186/1471-2105-14-346>.
- Demkowicz, W.E., Maa, J.S., Esteban, M., 1992. Identification and characterization of vaccinia virus genes encoding proteins that are highly antigenic in animals and are immunodominant in vaccinated humans. *J. Virol.* 66 (January (1)), 386–398.
- Drosten, C., Günther, S., Preiser, W., Van Der Werf, S., Brodt, H.R., Becker, S., Rabenau, H., Panning, M., Kolesnikova, L., Fouchier, R.A., Berger, A., 2003. Identification of a novel coronavirus in patients with severe acute respiratory syndrome. *N. Engl. J. Med.* 348 (May (20)), 1967–1976.
- Fehr, A.R., Perlman, S., 2015. Coronaviruses: an overview of their replication and pathogenesis. *Coronaviruses*. Humana Press, New York, NY, pp. 1–23.
- Gill, S.C., Von Hippel, P.H., 1989. Calculation of protein extinction coefficients from amino acid sequence data. *Anal. Biochem.* 182, 319–326. <https://doi.org/10.1093/oxfordjournals.jbchem.a133168>.
- Goerd, S., Orfanos, C.E., 1999. Other functions, other genes: alternative activation of antigen-presenting cells. *Immunity* 10, 137–142. [https://doi.org/10.1016/s1074-7613\(00\)80014-x](https://doi.org/10.1016/s1074-7613(00)80014-x).
- Hamre, D., Procknow, J.J., 1966. A new virus isolated from the human respiratory tract. *Proc. Soc. Exp. Biol. Med.* 121 (January (1)), 190–193.
- Hasson, S.S., Al-Busaidi, J.K., Sallam, T.A., 2015. The past, current and future trends in DNA vaccine immunisations. *Asian Pac. J. Trop. Biomed.* 5, 344–353. [https://doi.org/10.1016/s2221-1691\(15\)30366-x](https://doi.org/10.1016/s2221-1691(15)30366-x).
- Hopkins, Johns, 2020. University & medicine. Coronavirus Resource Center. March 29 Retrieved from. <https://coronavirus.jhu.edu/map.html>.
- Huang, C., Wang, Y., Li, X., Ren, L., Zhao, J., Hu, Y., Zhang, L., Fan, G., Xu, J., Gu, X., Cheng, Z., 2020. Clinical features of patients infected with 2019 novel coronavirus in Wuhan, China. *Lancet* 395 (February (10223)), 497–506.
- Ikai, A., 1980. Thermostability and aliphatic index of globular proteins. *J. Biochem.* 88, 1895–1898.
- Källberg, M., Wang, H., Wang, S., Peng, J., Wang, Z., Lu, H., Xu, J., 2012. Template-based protein structure modeling using the RaptorX web server. *Nat. Protoc.* 7, 1511. <https://doi.org/10.1038/nprot.2012.085>.
- Kaufmann, S.H., McElrath, M.J., Lewis, D.J., Del Giudice, G., 2014. Challenges and responses in human vaccine development. *Curr. Opin. Immunol.* 28, 18–26. <https://doi.org/10.1016/j.coi.2014.01.009>.
- Kovacs, J.A., Chacón, P., Abagyan, R., 2004. Predictions of protein flexibility: first-order measures. *Proteins: Struct. Funct. Bioinf.* 56, 661–668. <https://doi.org/10.1002/prot.20151>.
- Kyte, J., Doolittle, R.F., 1982. A simple method for displaying the hydropathic character of a protein. *J. Mol. Biol.* 157 (May (1)), 105–132.
- Laskowski, R.A., MacArthur, M.W., Moss, D.S., 1993. Thornton JM. PROCHECK: a program to check the stereochemical quality of protein structures. *J. Appl. Crystallogr.* 26, 283–291. <https://doi.org/10.1107/s0021889892009944>.
- López-Blanco, J.R., Garzón, J.L., Chacón, P., 2011. iMod: multipurpose normal mode analysis in internal coordinates. *Bioinformatics* 27, 2843–2850. <https://doi.org/10.1093/bioinformatics/btr497>.
- López-Blanco, J.R., Aliaga, J.I., Quintana-Ortí, E.S., Chacón, P., 2014. iMODS: internal coordinates normal mode analysis server. *Nucleic Acids Res.* 42, W271–6. <https://doi.org/10.1093/nar/gku339>.
- María, R.R., Arturo, C.J., Alicia, J.A., Paulina, M.G., Gerardo, A.O., 2017. The Impact of Bioinformatics on Vaccine Design and Development. *InTech, Rijeka, Croatia*. <https://doi.org/10.5772/intechopen.69273>. Sep 6.
- Masters, P.S., Perlman, S., 2013. Coronaviridae. *Fields Virol.* 1, 825–858.
- Merten, O.W., 2002. Virus contaminations of cell cultures—a biotechnological view. *Cytotechnology* 39, 91–116. <https://doi.org/10.1023/a:1022969101804>.
- Pace, C.N., Vajdos, F., Fee, L., Grimsley, G., Gray, T., 1995. How to measure and predict the molar absorption coefficient of a protein. *Protein Sci.* 4, 2411–2423. <https://doi.org/10.1002/pro.5560041120>.
- Pavli, P., Hume, D.A., Van De Pol, E., Doe, W.F., 1993. Dendritic cells, the major antigen-presenting cells of the human colonic lamina propria. *Immunology* 78, 132.
- Peeri, N.C., Shrestha, N., Rahman, M.S., Zaki, R., Tan, Z., Bibi, S., Baghbanzadeh, M., Aghamohammadi, N., Zhang, W., Haque, U., 2020. The SARS, MERS and novel coronavirus (COVID-19) epidemics, the newest and biggest global health threats: what lessons have we learned? *Int. J. Epidemiol.* (February), 22.
- Petit, C.M., Melancon, J.M., Chouljenko, V.N., Colgrove, R., Farzan, M., Knipe, D.M., Kousoulas, K.G., 2005. Genetic analysis of the SARS-coronavirus spike glycoprotein functional domains involved in cell-surface expression and cell-to-cell fusion. *Virology* 341 (October (2)), 215–230.
- Rottier, P.J., 1995. The coronavirus membrane glycoprotein. *The Coronaviridae*. Springer, Boston, MA, pp. 115–139.
- Sateesh, P., Rao, A., Sangeeta, S.K., Babu, M.N., Grandhi, R.S., 2010. Homology modeling and sequence analysis of anxC3. *Int. J. Eng. Sci. Technol.* 2, 1125–1130.
- Siu, K.L., Yuen, K.S., Castaño-Rodríguez, C., Ye, Z.W., Yeung, M.L., Fung, S.Y., Yuan, S., Chan, C.P., Yuen, K.S.Y., Enjuanes, L., Jin, D.Y., 2019. Severe acute respiratory syndrome coronavirus ORF3a protein activates the NLRP3 inflammasome by promoting TRAF3-dependent ubiquitination of ASC. *FASEB J.* 33 (August (8)), 8865–8877.
- Solanki, V., Tiwari, V., 2018. Subtractive proteomics to identify novel drug targets and reverse vaccinology for the development of chimeric vaccine against *Acinetobacter baumannii*. *Sci. Rep.* 8, 9044. <https://doi.org/10.1038/s41598-018-26689-7>.
- Stratton, K., Almario, D.A., McCormick, M.C., 2002. Institute of Medicine (US) Immunization Safety Review Committee. Immunization safety review: SV40

- contamination of polio vaccine and cancer. *Immunization Safety Review: SV40 Contamination of Polio Vaccine and Cancer*. National Academies Press, US.
- Su, S., Wong, G., Shi, W., Liu, J., Lai, A.C., Zhou, J., Liu, W., Bi, Y., Gao, G.F., 2016. Epidemiology, genetic recombination, and pathogenesis of coronaviruses. *Trends Microbiol.* 24 (June (6)), 490–502.
- Tameris, M.D., Hatherill, M., Landry, B.S., Scriba, T.J., Snowden, M.A., Lockhart, S., Shea, J.E., McClain, J.B., Hussey, G.D., Hanekom, W.A., Mahomed, H., 2013. Safety and efficacy of MVA85A, a new tuberculosis vaccine, in infants previously vaccinated with BCG: a randomised, placebo-controlled phase 2b trial. *Lancet* 381, 1021–1028. [https://doi.org/10.1016/s0140-6736\(13\)60177-4](https://doi.org/10.1016/s0140-6736(13)60177-4).
- Tanchot, C., Rocha, B., 2003. CD8 and B cell memory: same strategy, same signals. *Nat. Immunol.* 4, 431. <https://doi.org/10.1038/ni0503-431>.
- Thomsen, M., Lundegaard, C., Buus, S., Lund, O., Nielsen, M., 2013. MHCcluster, a method for functional clustering of MHC molecules. *Immunogenetics* 65, 655–665. <https://doi.org/10.1007/s00251-013-0714-0719>.
- Ullah, M.A., Sarkar, B., Islam, S.S., 2020a. Exploiting the Reverse Vaccinology Approach to Design Novel Subunit Vaccine against Ebola Virus. Manuscript submitted for publication. .
- Ullah, M.A., Sarkar, B., Islam, S.S., 2020b. Exploiting the reverse vaccinology approach to design novel subunit vaccine against ebola virus. medRxiv. <https://doi.org/10.1016/j.imbio.2020.151949>.
- van der Hoek, L., Pyrc, K., Jebbink, M.F., Vermeulen-Oost, W., Berkhout, R.J., Wolthers, K.C., Wertheim-van Dillen, P.M., Kaandorp, J., Spaargaren, J., Berkhout, B., 2004. Identification of a new human coronavirus. *Nat. Med.* 10 (April (4)), 368–373.
- Vita, R., Mahajan, S., Overton, J.A., Dhanda, S.K., Martini, S., Cantrell, J.R., Wheeler, D.K., Sette, A., Peters, B., 2018. The immune epitope database (IEDB): 2018 update. *Nucleic Acids Res.* (47), D339–343. <https://doi.org/10.1093/nar/gky1006>.
- Wang, C., Horby, P.W., Hayden, F.G., Gao, G.F., 2020. A novel coronavirus outbreak of global health concern. *Lancet* 395 (February (10223)), 470–473.
- Weiss, S.R., Navas-Martin, S., 2005. Coronavirus pathogenesis and the emerging pathogen severe acute respiratory syndrome coronavirus. *Microbiol. Mol. Biol. Rev.* 69 (December (4)), 635–664.
- World Health Organization, 2020. WHO Director-General's Opening Remarks at the Media Briefing on COVID-19-11 March 2020. March 11 Retrieved from: <https://www.who.int/dg/speeches/detail/who-director-general-s-opening-remarks-at-the-media-briefing-on-covid-19-11-march-2020>.
- Wu, C.Y., Monie, A., Pang, X., Hung, C.F., Wu, T.C., 2010. Improving therapeutic HPV peptide-based vaccine potency by enhancing CD4+ T help and dendritic cell activation. *J. Biomed. Sci.* 17 (88). <https://doi.org/10.1186/1423-0127-17-88>.
- Zaki, A.M., Van Boheemen, S., Bestebroer, T.M., Osterhaus, A.D., Fouchier, R.A., 2012. Isolation of a novel coronavirus from a man with pneumonia in Saudi Arabia. *N. Engl. J. Med.* 367 (November (19)), 1814–1820.
- Zobayer, M., 2018. In Silico Characterization and Homology Modeling of Histamine Receptors (Doctoral dissertation). Khulna University of Engineering & Technology (KUET), Khulna, Bangladesh. <https://doi.org/10.3923/jbs.2018.178.191>.